Full Paper

Synthesis and Pharmacological Screening of Novel *meso*-Substituted Porphyrin Analogs

Ahmed A. Fadda[1], Rasha E. El-Mekawy[1], Ahmed I. El-Shafei[2], and Harold Freeman[2]

[1] Faculty of Science, Department of Chemistry, Mansoura University, Mansoura, Egypt
[2] Polymer and Color Chemistry Program, North Carolina State University, Raleigh, NC, USA

A novel series of *meso*tetrakis[aryl]-21*H*,23*H*-porphyrin derivatives **2a–j** was synthesized from the condensation of aldehyde derivatives **1a–j** with pyrrole in the presence of *p*-toluenesulfonic acid. The synthesized porphyrins were considered as a model to study the free radical-induced damage of biological membranes and the protective effects of these porphyrins. It was found that these compounds effectively inhibit the free radical-induced oxidative hemolysis of red blood cells. Compounds **2c** and **2d** which bear a sulfur atom, a nitro group, and a chlorine atom exhibited markedly higher antihemolysis activity than the other analogous. Compounds **2a**, **2c**, **2d**, and **2j** showed the highest protection activity against DNA damage induced by the bleomycin–iron complex. Compounds **2d**, **2f**, **2i**, and **2j** were proved to exhibit antioxidative activity.

Keywords: Antioxidant / Cytotoxic and hemolysis activities / DNA damage / Porphyrins / UV spectra

Received: August 4, 2012; Revised: September 19, 2012; Accepted: September 26, 2012

DOI 10.1002/ardp.201200313

Introduction

Meso-substituted porphyrins have been widely used as key components in constructing porphyrin-based model systems as well as molecular materials [1, 2]. The design and synthesis of basic porphyrin building blocks for the construction of highly ordered systems often require incorporation of different peripheral substituents.

The synthesis of porphyrins bearing specific patterns of functionality is still a challenging task in spite of the ample presence of reported procedures [1]. The difficulties also arise from the separation, purification, and limited availability of suitable precursors. Although many sophisticated synthetic routes for designing porphyrins have been reported recently [3, 4], porphyrin building blocks bearing specific peripheral substituents are not available yet. Most of the reported methods generally adopted acid-catalyzed condensation of dipyrromethanes with appropriate aldehydes for the construction of porphyrins. Various new methodologies were developed. In the 1980s, a new approach for the synthesis of *meso*-substituted porphyrins under gentle conditions was developed, namely, two-step one-flask room temperature synthesis of porphyrins or the Lindsey method. Various facts were considered when designing the above-mentioned synthetic methodology. First, the Rothemund and Alder-Longo method employed harsh reaction conditions leading to the formation of porphyrins in low yields. In addition, the synthesis of porphyrins bearing sensitive functional groups could not be achieved. As a result of these drawbacks, the need to accomplish the condensation reaction under gentle conditions became an obvious requirement. Secondly, mild conditions were also desirable in order to avoid all the side reactions leading to undesired oligomers and side products. Recently, porphyrin nanoparticles were synthesized by ionic self-assembly in aqueous solutions of oppositely charged nonmetal porphyrin, namely anionic *meso*-tetra(4-sulfonatophenyl)porphine dihydrochloride ($TPPS_4$) and cationic *meso*-tetra(4-pyridyl)porphine (T_4MPyP) [5, 6].

Porphyrins have been reported to possess a variety of biological and pharmacological activities. The desirable cancer preventive or putative therapeutic properties of porphyrins have also been considered to be associated with their antioxidant properties, since free radical mediated peroxidation of membrane lipids and oxidative damage of DNA

Correspondence: Ahmed A. Fadda, Faculty of Science, Department of Chemistry, Mansoura University, El-Gomhoria Street, Mansoura 35516, Egypt.
E-mail: afadda50@yahoo.com
Fax: +20-50-2246781

were believed to be associated with a variety of chronic health problems, such as cancer, atherosclerosis, neurodegenerative diseases, and aging [7]. Therefore, the past few years have witnessed intense research devoted to the antioxidant activity of porphyrin. For instance, studies pertaining to the kinetics and mechanisms of natural antioxidants [8] have demonstrated that simple structural modifications of resveratrol, which is an antioxidative component in red wine, could significantly enhance its antioxidative activity [9] and cytotoxicity against cancer cells [10]. This motivated us to use porphyrin as a lead compound to design more active potential antioxidants and chemopreventive agents against cancer. We report herein the synthesis of a novel series of porphyrin analogs and an *in vitro* study of their protective effects on free radical-induced hemolysis of rat red blood cells (RBCs). RBC membranes are rich in polyunsaturated fatty acids which are very susceptible to free radical-mediated peroxidation, leading to damage of the membrane and hemolysis. The peroxidation was initiated by 2,2′-azo-*bis*(2-amidinopropane hydrochloride) (AAPH) which decomposes at physiological temperature and generates alkyl radicals to initiate lipid peroxidation (Eq. 1, *vide infra*). Since AAPH is water-soluble and the generation rate of free radicals from the decomposition of AAPH can be easily controlled and measured, it has been extensively used as a free radicals initiator for biological and related studies [11], and the AAPH-induced hemolysis provides a good experimental approach for studying free radical-induced membrane damage [12]. In order to broaden the scope and better understand the limitation of the synthesis of the model compounds, we have investigated the influence of several reaction parameters on the yields of porphyrins obtained. The reaction parameters included acid-catalyst, acid concentration, reactant concentrations, the added inorganic salts, and reaction times.

As their name origin from the Greek porphyra (purple) implies, typical porphyrins exhibit a deep-purple hue and all porphyrins are intensely colored. The electronic absorption spectra of conventional porphyrins, such as tetra *p*-methoxyphenyl porphyrin are characterized by a strong single band in the high-energy region of the visible spectrum ranging from 400 to 440 nm, referred to as the Soret or B band, and a series of bands appearing in the low-energy visible region from 500 to 700 nm, which are identified as the Q bands (Fig. 1). Both of these spectral features arise from π–π^* transitions and are described by the Gouterman [13] four orbital model. This paradigm invokes the two highest occupied molecular orbitals [a_{1u} (HOMO) and a_{2u} (HOMO-1)], which are of similar but distinct energies, and the two lowest, nearly degenerate, unoccupied molecular orbitals [e_{gy} (LUMO + 1) and e_{gx} (LUMO)], which are considered to have equal energies (Fig. 1).

Based upon this molecular orbital description, two bands of comparable energies in the reversible region are predicted ($a_{1u} \rightarrow e_g$ and $a_{2u} \rightarrow e_g$), but as observed in the spectrum of 5,10,15,20-*meso*tetrakis[*p*-methoxyphenyl]-21*H*,23*H*-porphyrin, the wavelengths of the two absorptions are quite dissimilar. This disparity has been attributed to a process known as configurational interaction, wherein the four orbitals combine to form three states (Fig. 1). Constructive interference arising from this hybridization provides the intense, high-energy Soret band from the $S_0 \rightarrow S_1$ absorption and destructive interference results in the Q bands from the $S_0 \rightarrow S_2$ absorption [14]. The multiple features observed in the latter have been attributed to a slight modification to this model which allows for two, rather than one, absorptions from two quasi-forbidden transitions and one vibrational satellite for each of these absorptions [15].

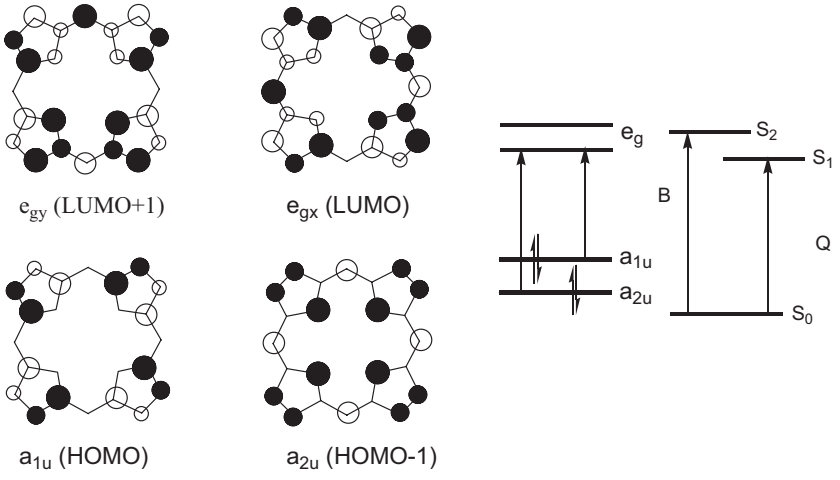

Figure 1. Illustration of the frontier orbitals, their relative energies and the states arising from configurational interactions of 5,10,15,20-*meso*tetrakis[3-nitrophenyl]-21*H*,23*H*-porphyrin [12].

Results and discussion

Although the synthesis of porphyrin derivatives has been previously reported [16, 17], we employed a new synthetic approach because of long-standing problems associated with low yield reactions, typically in the range of 6–20%, and purification using the published methods of Chan et al. [18]. They reported the purification using column chromatography on silica gel (3:1 dichloromethane/hexane), but the porphyrin product was not eluted under these conditions. Successive changes of the eluent to increasingly polar solvents were unsuccessful in moving the product in the column as well. The chromatographic conditions were therefore modified and successful purification was carried out on silica gel (1.5:1 chloroform/hexane). We developed a synthetic method that gave 72–81% yield with minimal chromatography. The key to our success was the use of a capping process that prevents the formation of polymeric pyrrole formation. Regarding the capping mechanism, we used DMF as a solvent to prevent the formation of polymeric pyrrole.

Meso-porphyrin derivatives **2a–j** were synthesized from the condensation of aldehyde derivatives **1a–j** with pyrrole in the presence of *p*-toluenesulfonic acid (Scheme 1). The yield and rate of condensation were found to depend on the concentration of *p*-toluenesulfonic acid, the solvent, the temperature, and the availability of atmospheric oxygen, and the

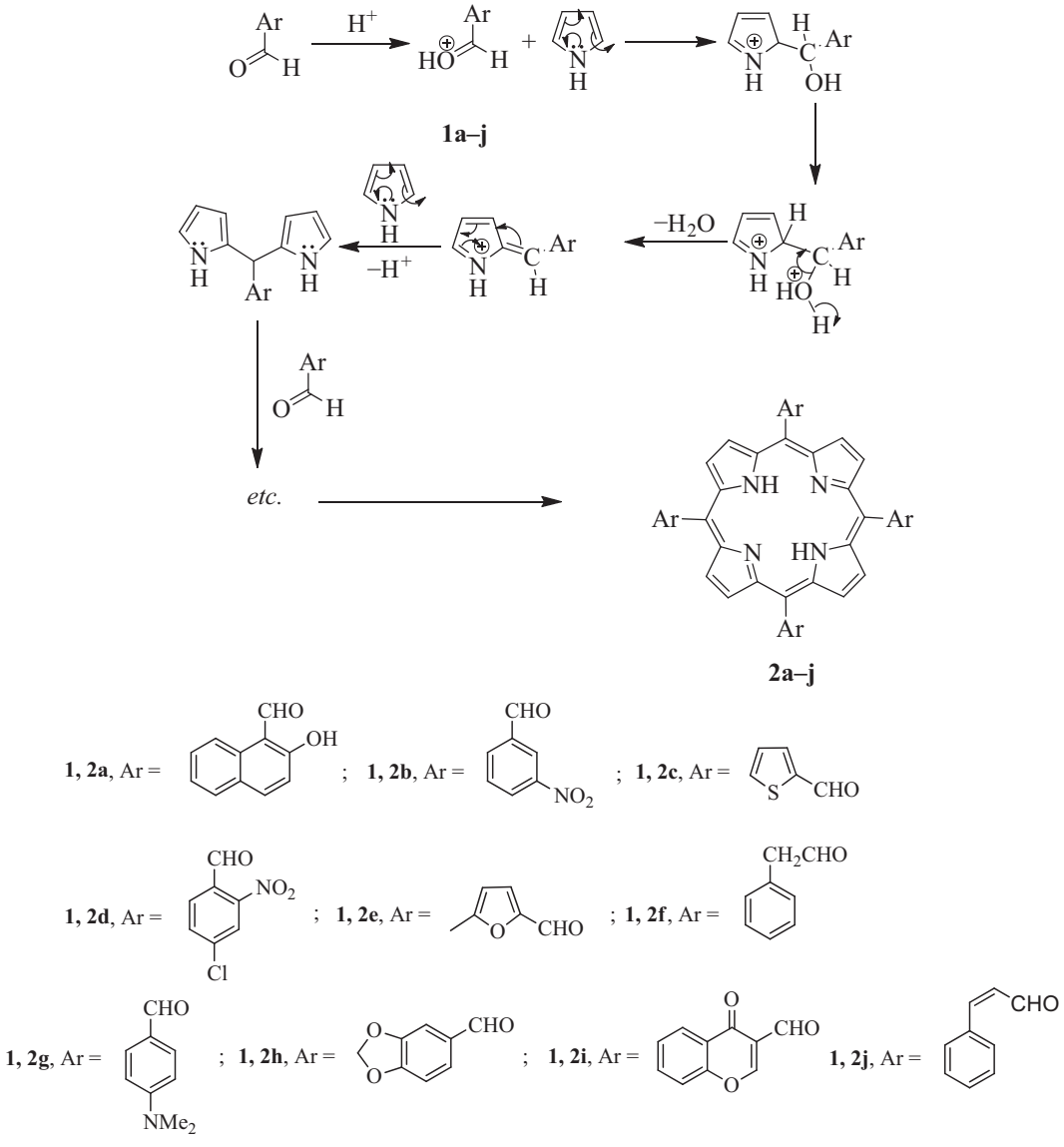

Scheme 1. Conventional synthetic route for the preparation of porphyrin derivatives **2a–j**.

initial concentration of the reactants. The porphyrin is the thermodynamic and the linear kinetic product and the mechanism of formation is shown in Scheme 1. It involves the acid-catalyzed addition of the pyrrole to the substituted benzaldehyde carbonyl group followed by acid-catalyzed dehydration. Repeating this process adds the next benzaldehyde moiety. Ring closure results in the formation of the reduced form of porphyrin (porphyrinogen) followed by oxidation to furnish the porphyrin building blocks. The proposed capping mechanism is shown in Scheme 2. In the presence of DMF, a reversible cap forms which protects this intermediate species, while allowing the reaction with pyrrole. If DMF or another solvent that can cap the reactive intermediate is not used as the solvent, this intermediate may react by polymerizing to generate a tarry substance or intractable mixture.

Among the investigated dyes, the relationship between the shifts observed in the absorption maximum given in Table 1 and the polar characteristics of the substituents may be summarized as follows: (i) Table 1 shows that the presence of electron donating or electron withdrawing groups did not bring about any marked increase or decrease in λ_{max} in the visible region and that log ε remained nearly constant. (ii) The introduction of an electron donating group in any position causes a bathochromic shift. This is clear from the absorption maximum of compounds **2a**–**j**. (iii) The introduction of an electron withdrawing group does not greatly alter the absorption maximum. However, it gives a better depth of color of the dyes as shown in Table 1.

Table 1. UV absorption bands of porphyrin derivatives **2a–j**.

Compound no.	λ_{max} (nm)	ε (cm^{-1} M^{-1})	log ε
2a	422	15000	4.17
2b	422	20000	4.30
2c	422	15000	4.17
2d	428	17000	4.23
2e	423	15000	4.17
2f	420	20000	4.30
2g	424	20000	4.30
2h	424	17000	4.23
2i	424	17000	4.23
2j	420	15000	4.17

Pharmacology

Bleomycin-dependent DNA damage

The bleomycins are a family of antitumor antibiotics, which are used routinely as antitumor agents. The bleomycin assay

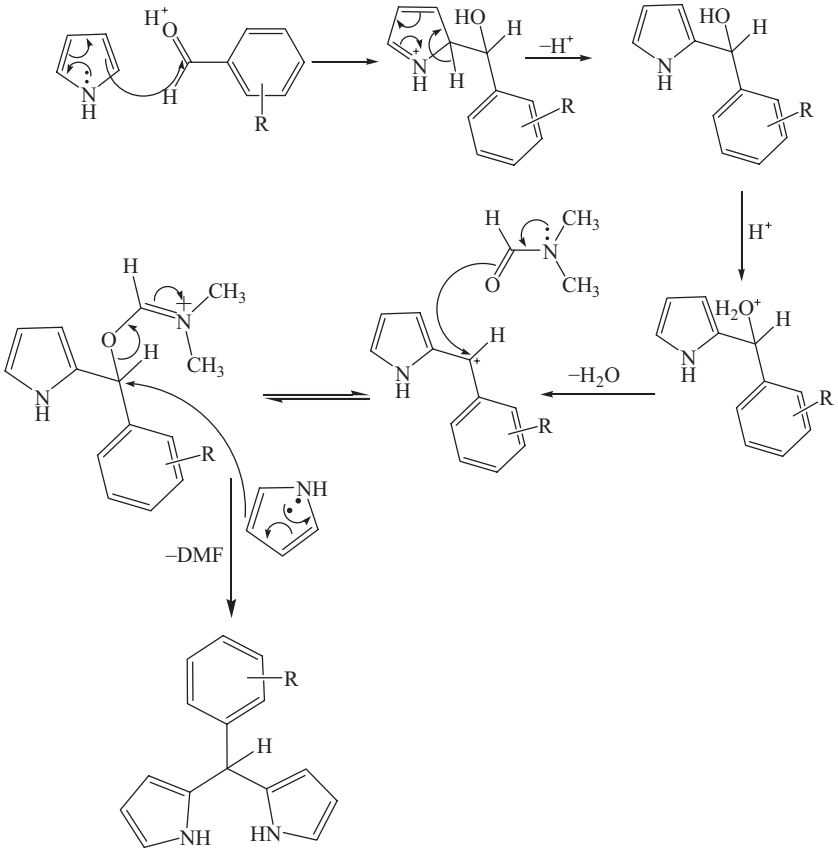

Scheme 2. Proposed role of DMF as a capping agent during porphyrin formation.

Table 2. Results of bleomycin-dependent DNA damage assay of isolated compounds.

Compound no.	Absorbance
2a	0.00882
2b	0.00858
2c	0.00886
2d	0.00886
2e	0.00851
2f	0.00920
2g	0.00821
2h	0.00984
2i	0.00893
2j	0.00883
L-Ascorbic acid	0.00881

has been adopted for assessing the pro-oxidant effects of food antioxidants. The antitumor antibiotic bleomycin binds iron ions and DNA. The resulting bleomycin–iron complex degrades DNA upon heating with thiobarbituric acid (TBA) yielding a pink chromogen. Added suitable reducing agents (''antioxidants'') compete with DNA and diminish chromogen formation.

Among all tested dyes (Table 2), compounds **2a**, **2c**, **2d**, and **2j** showed the highest protection activity against DNA damage induced by the bleomycin–iron complex, which diminished chromogen formation between the damaged DNA and TBA. However, compounds **2b**, **2e**, **2g**, and **2i** showed a weak to moderate activity, and compound **2f** and **2h** exhibited a very low activity.

Antioxidant activity using ABTS inhibition and erythrocyte hemolysis

All compounds were tested for antioxidant activity, which reflects the ability to inhibit peroxidation in rat brain and kidney homogenates and the rate of erythrocyte hemolysis. The antioxidant activities of the tested compounds were evaluated using the ABTS assay (Table 3). Compounds **2d**, **2f**, **2i**, and **2j** were proved to exhibit antioxidative activity. On the other hand, compounds **2a**, **2c**, and **2g** showed moderate activity, while compounds **2b**, **2e**, and **2h** showed weak activity.

Table 3. Antioxidant assay for the newly prepared compounds.

Compound no.	ABTS inhibition (%)	Erythrocyte hemolysis (%)
2a	73.67	1.01
2b	60.18	0.90
2c	73.70	0.89
2d	83.73	0.80
2e	18.60	1.90
2f	79.46	0.86
2g	74.38	0.91
2h	54.28	0.90
2i	79.46	0.86
2j	86.20	0.84
L-Ascorbic acid	88.61	0.85

AAPH-induced RBC hemolysis

Thermal decomposition of AAPH in the aqueous dispersion of RBCs produces an initiating radical ($R^\bullet$) which can attack the polyunsaturated lipids (LH) in RBC membranes to induce lipid peroxidation (Eqs. 1–6). The initiation rate of AAPH at 37°C in aqueous dispersions has been determined to be 1.3×10^{-6} [AAPH]/s. Since the lipid peroxidation is a free radical chain reaction and one initiating radical could induce up to 50 propagation reactions, the RBC membrane is quickly damaged, leading to hemolysis. On the other hand, if antioxidants (AH), such as vitamin E, vitamin C, and curcumin, are present or added to RBCs they would react with the chain-propagating peroxyl radicals to stop the peroxidation (Eq. 7), and hence inhibit hemolysis.

$$\text{Initiation:} \quad R-N=N-R \rightarrow 2R^\bullet + N_2 \tag{1}$$

$$R^\bullet + O_2 \rightarrow ROO^\bullet \tag{2}$$

$$ROO^\bullet + LH \rightarrow ROOH + L^\bullet \tag{3}$$

$$\text{Propagation:} \quad L^\bullet + O_2 \rightarrow LOO^\bullet \tag{4}$$

$$LOO^\bullet + LH \rightarrow LOOH + L^\bullet \tag{5}$$

$$\text{Termination:} \quad LOO^\bullet + LOO^\bullet \rightarrow \text{molecular products} \tag{6}$$

$$\text{Antioxidant:} \quad LOO^\bullet + AH \rightarrow LOOH + H^\bullet \tag{7}$$

Cytotoxicity

The synthesized compounds were evaluated and screened for cytotoxic activity (Table 4) against Vero (an African green monkey cell line), WI-38 (lung fibroblast cell line), HepG2 (hepatoma cells or human liver hepatocarcinoma cell line), and MCF-7 cells (human breast adenocarcinoma cell line; Fig. 2).

Dye **2j** exhibited the best cytotoxic activity against the HepG2 cell line, whereas, dyes **2d** and **2e** exhibited moderate cytotoxic activity against HepG2. Dyes **2a**, **2b**, **2c**, **2f**, **2g**, **2h**, and **2i** showed low activity against HepG2. By comparing the results of the tested compounds with **2j** we found that introduction of an ethylenic group enhances the activity against different cell lines.

Compound **2j** exhibited the best cytotoxic activity against the WI-38 cell line due to the presence of the ethylenic group which revealed a more potent activity. However, compound

Table 4. Cytotoxicity (IC_{50}) values of the tested compounds on different cell lines.

Compound no.	IC_{50}[a] (μg/ mL)			
	HepG2	WI-38	Vero	MCF-7
2a	88	87	84	84
2b	100	81	100	54
2c	83	100	87	39
2d	34	42	33	33
2e	44.5	59	56	80
2f	74	64	49	27
2g	64	74	56	54
2h	84	100	55	60
2i	76	64	65	74
2j	11	23	37	6
5-Fu[b]	9	0	7	0

[a] IC_{50} (μg/mL): 1–10 (very strong), 11–25 (strong), 26–50 (moderate), 51–100 (weak), 100–200 (very weak), 200 (non-cytotoxic).
[b] 5-Fu, 5-fluorouracil.

2d exhibited moderate cytotoxicity owing to the presence of a nitro group and a chlorine atom in the *ortho* and *para* positions, respectively, which act as electron withdrawing group, while the rest of the compounds showed weak activity.

On the other hand, compounds **2d**, **2j**, and **2f** showed moderate cytotoxic activity against the Vero cell line, whereas compounds **2a**, **2b**, **2c**, **2e**, **2g**, **2h**, and **2i** exhibited the lowest cytotoxic activity against the Vero cell line.

Furthermore, compound **2j** has an excellent ability for cytotoxic activity against MCF-7 cells due to the presence of an ethylenic group, whereas compounds **2c**, **2d**, and **2f** exhibited moderate cytotoxic activity against the MCF-7 cell line. Finally, compounds **2a**, **2b**, **2e**, **2g**, **2h**, and **2i** exhibited the lowest cytotoxic activity against the MCF-7 cell line.

Further *in vitro* studies are warranted to confirm the biological activity of the newly synthesized porphyrins and to investigate the molecular mechanisms responsible for the antitumor activity at the most compounds with a potential pharmaceutical use.

Experimental

All melting points were uncorrected in degree centigrade and determined on a Gallenkamp electric melting point apparatus. The IR spectra were recorded (KBr disk) on a Mattson 5000 FTIR spectrometer at the Faculty of Science, Mansoura University. The ^{1}H NMR spectra were measured on a Bruker WP 300, 200 MHz in DMSO and $CDCl_3$ as solvents using TMS as internal standard at the Microanalytical Center, Faculty of Science, Cairo University. Ultraviolet spectra were carried out using a Unicam UV/Vis spectrometer at the Microanalytical Unit, Chemistry Department, Faculty of Science, Mansoura University. The starting materials for synthesis were obtained from Aldrich Chemical Company unless otherwise stated. Pyrrole was distilled under argon with the fraction boiling at 140°C collected. 2-Formyl benzene sulfonic acid sodium salt was purified using the Dean and Stark method and benzene as solvent. The solution was filtered at 60°C and the solid was pumped in a vacuum oven overnight at room temperature. *N*,*N*-Dimethylformamide (99.9% anhydrous grade) was used without further purification. *p*-Toluenesulfonic acid was purified by Dean and Stark method using benzene as solvent.

Chemistry

*Synthesis of porphyrin derivatives **2a–i***

General procedure: A mixture of the appropriate aromatic aldehyde (1.44 mmol), pyrrole (1.44 mmol, 0.0967 g) in DMF (10 mL) was placed into a 100 mL three necked round-bottom flask fitted with magnetic stirrer, condenser equipped with a Dean-Stark trap, thermometer, and argon gas bubbler inlet tube. The reaction mixture was flushed with argon for 5 min and then heated to 100°C for 10 min. Toluene sulfonic acid (1.44 mmol, dissolved in 5 mL DMF) was added to the reaction mixture using a syringe. The clear, colorless reaction mixture turned various shades of red over the next 1–2 min, and was heated to 150°C and held at this temperature for 1 h. Aliquots were removed from the reaction mixture to monitor it by UV–Vis. UV–Vis and DMF solutions showed the first product in the reaction to absorb at 504 nm (Q band). On continued heating at 150°C, the Soret band of porphyrins (λ_{max} 415–430 nm) continued to grow with continuous decline in the Q band intensity. After 1 h at 150°C, the reaction mixture was cooled in an ice bath for 20 min and then poured into ice-water. The precipitate was collected by filtration, dried under vacuum at ambient temperature, and the residue was

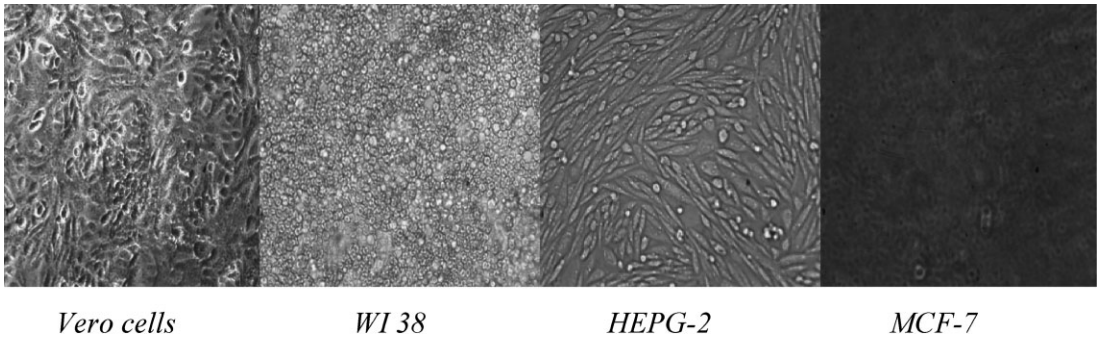

Figure 2. Confluent monolayers of the cell lines used for testing.

purified by column chromatograghy (silica gel, chloroform/hexane 1.5:1 as eluent).

*5,10,15,20-Mesotetrakis[2-hydroxynaphthayl]-21H,23H-porphyrin (**2a**)*

Yield 73.51%; black crystals; m.p. 100°C; IR (KBr): υ/cm^{-1} = 3394 (OH), 3235 (NH), 1654 (C=C), 1623 (C=N); ^{1}H NMR (DMSO-d_6) δ (ppm): 2.28 (s, 1H, NH), 5.20 (d, 2H, 2 pyrrolic CH), 6.30 (d, 2H, 2 pyrrolic CH), 7.10 (d, 2H, 2 pyrrolic CH), 7.25 (d.d, 4H, Ar–H), 7.37 (d, 4H, Ar–H), 7.41 (d, 4H, Ar–H), 7.46 (d, 2H, 2 pyrrolic CH), 7.66 (d, 4H, Ar–H), 7.77 (d.d, 4H, Ar–H), 7.94 (s, 4H, 4 OH), 8.11 (d, 4H, Ar–H), 10.10 (s, 1H, NH); UV–Vis spectrum: (λ_{max}), 422 nm. Anal. calcd. for $C_{60}H_{38}N_4O_4$ (878): C, 81.99; H, 4.36; N, 6.37%. Found: C, 82.00; H, 4.38; N, 6.38%.

*5,10,15,20-Mesotetrakis[3-nitrophenyl]-21H,23H-porphyrin (**2b**)*

Yield 80%; black crystals; m.p. 190°C; IR (KBr): υ/cm^{-1} = 3396 (NH), 1660 (C=C), 15 277 (C=N), 1348–1527 (NO_2); ^{1}H NMR (DMSO-d_6) δ (ppm): 2.28 (s, 1H, NH), 5.2 (d, 2H, 2 pyrrolic CH), 6.22 (d, 2H, 2 pyrrolic CH), 7.10 (d, 2H, 2 pyrrolic CH), 7.45 (d, 2H, 2 pyrrolic CH), 7.95 (s, 4H, Ar–H), 8.10 (d, 4H, Ar–H), 8.70 (d.d, 4H, Ar–H), 8.97 (d, 4H, Ar–H), 10.60 (s, 1H, NH); ^{13}C NMR (DMSO-d_6) δ (ppm): 161.18, 155.89, 147.86, 140.98, 137.78, 136.56, 133.43, 132.23, 129.98, 125.1, 123.37, 122.98, 120.59, 119.96, 103.05; UV–Vis spectrum: (λ_{max}), 422 nm. Anal. calcd. for $C_{40}H_{26}N_5O_2$ (608): C, 66.70; H, 3.30; N, 14.10%. Found: C, 66.70; H, 3.32; N, 14.11%.

*5,10,15,20-Mesotetrakis[2-thienyl]-21H,23H-porphyrin (**2c**)*

Yield 72%; brown crystals; m.p. 140°C; IR (KBr): υ/cm^{-1} = 3413 (NH), 1654 (C=N), 1554 (C=C); ^{1}H NMR (DMSO-d_6) δ (ppm): 2.30 (s, 1H, NH), 5.75 (d, 2H, 2 pyrrolic CH), 5.89 (d, 2H, 2 pyrrolic CH), 7.10 (d, 2H, 2 pyrrolic CH), 7.45 (d, 2H, 2 pyrrolic CH), 7.72 (d.d, 2H, 4 thiophenic CH), 8.05 (d, 2H, 4 thiophenic CH), 8.20 (d, 2H, 4 thiophenic CH), 10.60 (s, 1H, NH); UV–Vis spectrum: (λ_{max}), 422 nm. Anal. calcd. for $C_{36}H_{22}N_4S_4$ (638): C, 67.71; H, 3.45; N, 8.77%. Found: C, 67.74; H, 3.45; N, 8.78%.

*5,10,15,20-Mesotetrakis[4-chloro-2-nitrophenyl]-21H,23H-porphyrin (**2d**)*

Yield 81%; deep reddish brown powder; m.p. >300°C; IR (KBr): υ/cm^{-1} = 3419 (NH), 1602 (C=C), 1509 (C=N), 819 (C–Cl); ^{1}H NMR (DMSO-d_6) δ (ppm): 2.28 (s, 1H, NH), 6.64 (d, 1H, 2 pyrrolic CH), 6.84 (d, 2H, 2 pyrrolic CH), 6.95 (d, 2H, 2 pyrrolic CH), 7.10 (d, 2H, 2 pyrrolic CH), 7.46 (d, 2H, Ar–H), 7.78 (d, 4H, Ar–H), 7.90 (s, 4H, Ar–H), 10.55 (s, 1H, NH); ^{13}C NMR (DMSO-d_6) δ (ppm): 161.23, 146.29, 136.43, 134.62, 134.37, 131.33, 128.61, 125.0, 124.16, 122.97, 120.36, 103.34; UV–Vis spectrum: (λ_{max}), 428 nm. Anal. calcd. for $C_{44}H_{22}N_8O_8Cl_4$ (932.51): C, 56.65; H, 2.36; N, 12.01%. Found: C, 56.57; H, 2.35; N, 12.01%.

*5,10,15,20-Mesotetrakis[5-methyl-2-furfuryl]-21H,23H-porphyrin (**2e**)*

Yield 72%; deep brown crystals; m.p. 170°C; IR (KBr): υ/cm^{-1} = 3419 (NH), 2919 (CH_3), 1612 (C=C), 1563 (C=N); ^{1}H NMR (DMSO-d_6) δ (ppm): 2.28 (s, 12H, 4 CH_3), 3.83 (s, 1H, NH), 5.90 (d, 2H, 2 pyrrolic CH), 6.38 (d, 4H, 4CH), 6.62 (d, 2H, 2 pyrrolic CH), 6.98 (d, 2H, 2 pyrrolic CH), 7.11 (d, 21H, 4 CH), 7.48 (d, 2H, 4CH), 10.59 (s, 1H, NH); UV–Vis spectrum: (λ_{max}), 423 nm. Anal. calcd. for $C_{40}H_{30}N_4O_4$ (630): C, 76.19; H, 4.76; N, 8.89%. Found: C, 76.20; H, 4.77; N, 8.90%.

*5,10,15,20-Tetrabenzyl-21H,23H-porphyrin (**2f**)*

Yield 75.8%; brown crystals; m.p. 120°C; IR (KBr): υ/cm^{-1} = 3419 (NH), 2923 (CH_2), 1594 (C=C), 1560 (C=N); ^{1}H NMR (DMSO-d_6) δ (ppm): 2.25 (s, 8H, 4 CH_2), 3.89 (s, 1H, NH), 5.24 (d, 1H, 2 pyrrolic CH), 6.18 (d, 2H, 2 pyrrolic CH), 6.88 (d, 2H, 2 pyrrolic CH), 6.98 (d, 2H, 2 pyrrolic CH), 7.30 (d.d, 8H, Ar–H), 7.43 (d.d, 4H, Ar–H), 7.52 (d.d, 4H, Ar–H), 7.77 (d, 4H, Ar–H), 7.94 (d, 1H, Ar–H), 10.50 (s, 1H, NH); UV–Vis spectrum: (λ_{max}), 420 nm. Anal. calcd. for $C_{48}H_{38}N_4$ (670): C, 85.94; H, 5.71; N, 8.35%. Found: C, 85.95; H, 5.71; N, 8.36%.

*5,10,15,20-Mesotetrakis[4-N,N-dimethylaminophenyl]-21H,23H-porphyrin (**2g**)*

Yield 80.10%; deep violet crystals; m.p. >300°C; IR (KBr): υ/cm^{-1} = 3409 (NH), 2923 ($2CH_3$), 1602 (C=C), 1519 (C=N); ^{1}H NMR (DMSO-d_6) δ (ppm): 3.02 (s, 1H, NH), 3.89 (s, 24H, 4 N-$(CH_3)_2$), 5.3 (d, 2H, 2 pyrrolic CH), 6.2 (d, 2H, 2 pyrrolic CH), 6.44 (d, 2H, 2 pyrrolic CH), 6.51 (d, 2H, 2 pyrrolic CH), 6.94 (d, 8H, Ar–H), 7.27 (d, 8H, Ar–H), 10.22 (s, 1H, NH); UV–Vis spectrum: (λ_{max}), 424 nm. Anal. calcd. for $C_{52}H_{50}N_8$ (786): C, 79.36; H, 4.40; N, 14.24%. Found: C, 80.00; H, 4.41; N, 14.25%.

*5,10,15,20-Mesotetrakis[5-(benzo[d][1,3]dioxolyl)]-21H,23H-porphyrin (**2h**)*

Yield 73%; black crystals; m.p. 162°C; IR (KBr): υ/cm^{-1} = 3419 (NH), 2923 (CH_2), 1596 (C=C), 1560 (C=N); ^{1}H NMR (DMSO-d_6) δ (ppm): 3.78 (s, 1H, NH), 5.22 (d, 2H, 2 pyrrolic CH), 5.60 (d, 2H, 2 pyrrolic CH), 5.90 (s, 8H, 4 CH_2), 6.34 (s, 2H, Ar–H), 6.67 (d, 2H, 2 pyrrolic CH), 6.78 (d, 2H, 2 pyrrolic CH), 7.10 (d, 2H, Ar–H), 7.35 (d, 2H, Ar–H), 7.49 (d, 2H, Ar–H), 7.62 (d, 2H, Ar–H), 7.95 (s, 1H, Ar–H), 10.44 (s, 1H, NH); UV–Vis spectrum: (λ_{max}), 424 nm. Anal. calcd. for $C_{52}H_{30}N_4O_8$ (838): C, 74.46; H, 3.58; N, 6.68%. Found: C, 74.47; H, 3.60; N, 6.70%.

*5,10,15,20-Mesotetrakis[3-(4-oxo-4H-chromenyl]-21H,23H-porphyrin (**2i**)*

Yield 79.32%; deep blackish red crystals; m.p. 230°C; IR (KBr): υ/cm^{-1} = 3409 (NH), 1690 (C=O), 1612 (C=C), 1554 (C=N); ^{1}H NMR (DMSO-d_6) δ (ppm): 2.28 (s, 1H, NH), 5.62 (d, 2H, 2 pyrrolic CH), 5.81 (d, 2H, 2 pyrrolic CH), 6.59 (d, 2H, 2 pyrrolic CH), 7.09 (d, 2H, 2 pyrrolic CH), 7.46 (d, 4H, Ar–H), 7.61 (d, 4H, Ar–H), 7.76 (d.d, 4H, Ar–H), 7.95 (s, 4H, 4 CH), 8.09 (d.d, 4H, Ar–H), 10.59 (s, 1H, NH). ^{13}C NMR (DMSO-d_6) δ (ppm): 177.49, 157.55, 149.33, 147.16, 138.49, 135.0, 133.65, 129.48, 125.30, 123.55, 122.99, 119.95, 117.08, 115.90; UV–Vis spectrum: (λ_{max}), 424 nm. Anal. calcd. for $C_{56}H_{30}N_4O_8$ (868): C, 77.42; H, 3.45; N, 6.45%. Found: C, 77.44; H, 3.50; N, 6.45%.

*10,15,20-Mesotetrakis[phenylethylene]-21H,23H-porphyrin (**2j**)*

Yield 82%; brown powder; m.p. >300°C; IR (KBr): υ/cm^{-1} = 3429 (NH), 3052 (=CH), 1612 (C=N), 1554 (C=C); ^{1}H NMR (DMSO-d_6) δ (ppm): 2.3 (s, 1H, NH), 5.41 (d, 2H, 2 pyrrolic CH), 5.65 (d, 2H, 2 pyrrolic CH), 5.90 (d, 2H, 2 pyrrolic CH), 6.12 (d, 2H, 2 pyrrolic CH), 6.65 (s, 1H, CH), 6.85 (s, 1H, CH), 7.01–7.54 (m, 20H, Ar–H),

10.60 (s, 1H, NH); UV–Vis spectrum: (λ_{max}), 420 nm. Anal. calcd. for $C_{52}H_{38}N_4$ (718): C, 86.88; H, 5.33; N, 7.79%. Found: C, 86.90; H, 5.34; N, 7.81%.

Biological activity

Reagents

DNA (Type 1. Calf Thymus), bleomycin sulfate, butylated hydroxyanisole (BHA), and L-ascorbic acid were purchased from Sigma Company. 2,2′-Azo-*bis*-(2-amidinopropane) dihydrochloride (AAPH), 2,2′-azino-*bis*(3-ethyl benzthiazoline-6-sulfonic acid) (ABTS) were purchased from Wak. All other chemicals were of analytical grade.

Antioxidant activity screening assay for erythrocyte hemolysis

Blood was obtained from rats by cardiac puncture and collected in heparinized tubes. Erythrocytes were separated from plasma and the buffy coat and washed three times with 10 volumes of 0.15 M NaCl. During the last washing, the erythrocytes were centrifuged at 2500 rpm for 10 min to obtain a constantly packed cell preparation. Erythrocyte hemolysis was mediated by peroxyl radicals in this assay system. A 10% suspension of erythrocytes in phosphate buffered saline pH 7.4 (PBS) was added to the same volume of 200 mM 2,2′-azo*bis*(2-amidinopropane) dihydrochloride (AAPH) solution (in PBS) containing samples to be tested at different concentrations. The solution was shaken gently while being incubated at 37°C for 2 h, diluted with eight volumes of PBS and centrifuged at 1500*g* for 10 min. The absorbance A of the supernatant was measured at 540 nm. Similarly, the reaction mixture was treated with eight volumes of distilled water to achieve complete hemolysis, and the absorbance B of the supernatant obtained after centrifugation was measured at 540 nm [19]. The percentage hemolysis data was expressed as mean ± standard deviation. L-Ascorbic acid was used as a positive control.

Antioxidant activity screening assay ABTS method

For each of the investigated dyes, 2 mL of ABTS solution (60 μM) was added to 3 mL MnO_2 solution (25 mg/mL) all prepared in 5 mL aqueous phosphate buffer solution (pH 7, 0.1 M). The mixture was shaken, centrifuged, filtered, and the absorbance (A control) of the resulting green-blue solution (ABTS radical solution) at λ_{max} 734 nm was adjusted at approx. 0.5. Then, 50 μL of 2 mL solution of the test compound in spectroscopic grade MeOH/phosphate buffer (1:1) was added. The absorbance (A test) was measured and the reduction in color intensity was expressed as % inhibition percentage. L-Ascorbic acid (vitamin C) was used as standard antioxidant (positive control), and a blank sample was run without ABTS and using MeOH/phosphate buffer (1:1) instead of the tested compounds. Negative control was run with ABTS phosphate buffer (1:1) only [20].

Bleomycin-dependent DNA damage assay

The reaction mixtures contained, in a final volume of 1.0 mL, the following reagents at the final concentrations stated: DNA (0.2 mg/ mL), bleomycin (0.05 mg/mL), $FeCl_3$ (0.025 mM), MgCl (5 mM), KH_2PO_4–KOH buffer pH 7.0 (30 mM), and ascorbic acid (0.24 Mm) or the dyes tested in MeOH to give a concentration of (0.1 mg/mL). The reaction mixtures were incubated in a water bath at 37°C for 1 h. At the end of the incubation period, 0.1 mL of 0.1 M EDTA was added to stop the reaction (the iron–EDTA complex is unreactive in the bleomycin assay). DNA damage was assessed by adding 1 mL 1% w/v TBA and 1 mL 25% v/v hydrochloric acid (HCl) followed by heating in a water bath maintained at 80°C for 15 min. The chromogen formed was extracted into butan-1-ol and the absorbance was measured at 532 nm [21, 22].

Cytotoxicity and antitumor assay

Samples were prepared for assay by dissolving test dyes in 50 μL of DMSO and diluting aliquots into sterile culture medium at 0.4 mg/mL. These solutions were subdiluted to 0.02 mg/mL in sterile medium and the two solutions used as stocks to test samples at 100, 50, 20, 10, 5, 2, and 1 mg/mL in triplicate in the wells of microtiter plates.

The tested dyes **2a–j** were assayed in triplicate on monolayers grown in Dulbecco's modified Eagle's medium supplemented with 10% v/v calf serum (Hyclone Laboratories, Ogden, UT), 60 mg/mL pencillin G and 100 mg/mL streptomycin sulfate maintained at 37°C in a humidified atmosphere containing about 15% v/v CO_2 in air. All medium components were obtained from Sigma Chemical Co., St. Louis, MO, unless otherwise indicated. Cells stocks were maintained at 34°C in culture flasks filled with medium supplemented with 1% v/v calf serum. Subcultures of cells for screening were grown in the wells of microtiter trays (Falcon Microtest III 96-wells trays, Becton Dickinson Labware, Lincolin Park, NJ) by suspending cells in medium following trypsin–EDTA treatment, counting the suspension with a hemocytometer, diluting in medium containing 10% calf serum to 2×10^4 cells per 200 mL culture, aliquoting into each well of a tray and culturing until confluent.

Microtiter trays with confluent monolayer cultures of cells were inverted, the medium shaken out, and replaced with serial dilutions of sterile dyes in triplicate in 100 μL medium followed by titered virus in 100 μL medium containing 10% v/v calf serum in each well. In each tray, the last row of wells was reversed for controls that were not treated with dyes. The trays were cultured for 96 h. The trays were inverted onto a pad of paper towels, the remaining cells rinsed carefully with medium and fixed with 3.7% v/v formaldehyde in saline for at least 20 min. The fixed cells were rinsed with water and examined visually. The cytotoxic activity is identified as confluent, relatively unaltered monolayers of stained cells treated with compounds. Cytotoxicity was estimated as the concentration that caused approximately 50% loss of the monolayer. 5-Fluorouracil was used as a positive control [23].

To Prof. Dr. Farid A. Badria, Professor of Pharmacognosy, Faculty of Pharmacy, Mansoura University, for biological activity screening of the tested compounds.

The authors have declared no conflict of interest.

References

[1] For the general review, see: (a) J. S. Lindsey, Synthesis of meso-Substituted Porphyrins, in *The Porphyrin Handbook* (Eds.: K. M. Kanish, K. M. Smith, R. Guilard), Academic Press, San Diego, **2000**, Chapter 2, pp. 45–118; (b) D. Holten, D. F. Bocian, J. S. Lindsey, *Acc. Chem. Res.* **2002**, *35*, 57–69.

[2] (a) A. Nakano, A. Osuka, I. Yamazaki, T. Yamazaki, Y. Nishimura, *Angew. Chem. Int. Ed. Engl.* **1998**, *37*, 3023–3027; (b) O. Mongin, A. Schuwey, M. A. Vallot, A. Gossauer, *Tetrahedron Lett.* **1999**, *40*, 8347–8350.

[3] (a) Z. Yao, J. Bhaumik, S. Dhanalekshmi, M. Ptaszek, P. A. Rodriguez, J. S. Lindsey, *Tetrahedron* **2007**, *63*, 10657–10670; (b) J. Bhaumik, Z. Yao, K. E. Borbas, M. Taniguchi, J. S. Lindsey, *J. Org. Chem.* **2006**, *71*, 8807–8817; (c) K. Padmaja, W. J. Youngblood, L. Wei, D. F. Bocian, J. S. Lindsey, *Inorg. Chem.* **2006**, *45*, 5479–5492.

[4] (a) K. Muthukumaran, R. S. Loewe, A. Amroise, S. Tamaru, Q. Li, G. Mathur, D. F. Bocian, V. Misra, J. S. Lindsey, *J. Org. Chem.* **2004**, *69*, 1444–1452; (b) A. Balakumar, A. B. Lysenko, C. Carcel, V. L. Malinovskii, D. T. Gryko, K. Schweikart, R. S. Loewe, A. A. Yasseri, Z. Liu, D. F. Bocian, J. S. Lindsey, *J. Org. Chem.* **2004**, *69*, 1435–1443; (c) L. Wei, K. Padmaja, W. J. Youngblood, A. B. Lsenko, J. S. Lindsey, D. F. Bocian, *J. Org. Chem.* **2004**, *69*, 1461–1469.

[5] M. M. Kashani-Motlagh, R. Rahmatollah, M. J. Kachousangi, *Molecules* **2010**, *15*, 280–287.

[6] S. Valentinas, V. Mizariene, *Int. J. Nanomanuf.* **2010**, *5*, 194–204.

[7] K. J. Barnham, C. L. Masters, A. I. Bush, *Nat. Rev. Drug Discov.* **2004**, *3*, 205–214.

[8] (a) M. S. Cooke, M. D. Evans, M. Dizdaroglu, J. Lunez, *FASEB J.* **2003**, *17*, 1195–1214; (b) T. Finkel, N. G. Holbrook, *Nature* **2000**, *408*, 239–247; (c) S. P. Hussain, L. J. Hofseth, C. C. Harris, *Nat. Rev. Cancer* **2003**, *3*, 276–285.

[9] (a) Y.-J. Cai, L. P. Ma, L. F. Hou, B. Zhou, L. Yang, Z.-L. Liu, *Chem. Phys. Lipids* **2002**, *120*, 109–117; (b) Z.-H. Chen, B. Zhou, L. Yang, L.-M. Wu, Z.-L. Liu, *J. Chem. Soc, Perkin Trans. 2* **2001**, 1835–1839, DOI: 10.1039/B101713F; (c) B. Zhou, Q. Miao, L. Yang, Z.-L. Liu, *Chem. Eur. J.* **2005**, *11*, 680–691; (d) B. Zhou, L.-M. Wu, L. Yang, Z.-L. Liu, *Free Radical Biol. Med.* **2005**, *38*, 78–84.

[10] Y. J. Cai, J. G. Fang, L. P. Ma, L. Yang, Z.-L. Liu, *Biochim. Biophys. Acta* **2003**, *1637*, 31–38.

[11] Y. J. Cai, Q. Y. Wei, J. G. Fang, L. Yang, Z. L. Liu, J. H. Wyche, Z. Han, *Anticancer Res.* **2004**, *24*, 999–1002.

[12] (a) L. Hou, B. Zhou, L. Yang, Z.-L. Liu, *Chem. Phys. Lipids* **2004**, *129*, 209–219; (b) L. Hou, B. Zhou, L. Yang, Z.-L. Liu, *Org. Biomol. Chem.* **2004**, *2*, 1419–1423.

[13] M. Gouterman, The Q bands in the absorption spectra are quenched, in *The Porphyrins*, Vol. III (Ed.: D. Dolghin), Academic Press, New York **1978**.

[14] H. L. Anderson, *Chem. Commun.* **1999**, 2323–2330.

[15] N. Z. Mamardashvili, O. A. Golubchikov, *Uspekhi Khim.* **2001**, *70*, 656.

[16] H. Tang, Z. Dong, Z. Merican, D. Margetić, Z. Marinić, M. J. G. David officer, D. N. Butler, R. N. Warrener, *Tetrahedron Lett.* **2009**, *50*, 667–670.

[17] S. Rai, M. Ravikanth, *J. Org. Chem.* **2008**, *73*, 8364–8375.

[18] C.-S. Chan, A. K.-S. Tse, K. S. Chan, *J. Org. Chem.* **1994**, *59*, 6084–6089.

[19] Y. Morimoto, K. Tanaka, Y. Iwakiri, S. Tokuhiro, S. Fukushima, Y. Takeuchi, *Biol. Pharm. Bull.* **1995**, *18*, 1417–1422.

[20] A. B. A. El-Gazzar, A. M. S. Youssef, M. M. Youssef, A. A. Abu-Hashem, F. A. Badria, *Eur. J. Med. Chem.* **2009**, *44*, 609–624.

[21] J. Gutteridge, D. Rowley, B. Halliwel, *Biochem. J.* **1981**, *199*, 263–265.

[22] B. F. Abdel-Wahab, A.-A. S. El-Ahl, F. A. Badria, *Chem. Pharm. Bull.* **2009**, *57*, 1348–1351.

[23] H. El-Subbagh, M. Abu-Zaid, M. Mahran, F. Badria, A. Al-Obaid, *J. Med. Chem.* **2000**, *43*, 2915–2921.

